Available online at www.sciencedirect.com
ScienceDirect
Journal of Nuclear Materials 374 (2008) 344–353
journal of nuclear materials
www.elsevier.com/locate/jnucmat

A plutonium α-decay defects production study through displacement cascade simulations with MEAM potential

L. Berlu [a], G. Jomard [b,*], G. Rosa [a], P. Faure [a]

[a] CEA Valduc, F-21120 Is Sur Tille, France
[b] CEA – Bruyères le Châtel, F-91680 Bruyères le Châtel, France

Received 27 May 2007; accepted 12 September 2007

Abstract

This paper presents results of molecular dynamics simulations of self-irradiation in δ-Pu. The goal of this work is to understand, at an atomistic level, phenomena that lead to the experimentally observed swelling of plutonium-based materials. In a first step, we have performed a parametric study including both potential formalism, simulation cell size, temperature and cascade energy. The comparison of the EAM (Embedded Atom Method) and the MEAM (Modified Embedded Atom Method) shows that the behavior of displacement cascades in δ-Pu is strongly sensitive to the interaction model. Our calculations reveal that the development of a collision cascade in δ-Pu is highly different from what is known for other face-centered-cubic metals. We observe that the disordered region induced by the melting of the cascade core is curiously stable for tens of nanoseconds. The causes of this unusual behavior are examined on the basis of the above-mentioned parametric study.

1. Introduction

The radioactivity of plutonium is expressed essentially through α-decay, leading to the creation of high energy nuclei of uranium (86 keV) and helium (5 MeV). These particles can displace plutonium atoms from their equilibrium sites through collisions. Resulting displacement cascades are then the source of numerous point defects in the metal structure. These defects and their clusters are susceptible to cause important problems in materials properties. Experimental measurements have indeed shown that plutonium structure could be affected by radiation damages. As an example, swelling of plutonium alloys has been observed during aging with different techniques (dilatometry, X-ray diffraction) [1–4]. Such modifications and their consequences are not yet well understood and need to be studied. To overcome difficulties imposed by plutonium radioactivity and toxicity, computer simulation is of great interest. For this reason we have developed a multi-scale modelling study of plutonium aging. The aim of this program is to predict the evolution of plutonium alloys properties over years. Its success requires the knowledge of the main physical processes occurring during aging; then it combines simulation methods ranging from the atomic scale with first-principles calculations to the macroscopic scale with kinetic rate modelling [4,5]. Displacement cascades occur over length and time scales that are tractable for atomic scale simulations. They lead to the creation of many types of defects. To understand the physical phenomena appearing at this scale, a parametric study of molecular dynamics (MD) simulations of displacement cascades has been initiated.

The efficiency of molecular modelling depends on the ability of the interatomic potential to capture physical properties of the materials of interest. Numerous results in various systems clearly show that cascades induce melting of the material during the collision stage before recrystallization [6–10] or amorphization [11–13] takes place from relaxation of defects.

To achieve reliable simulations, the interatomic potential must predict, with respect to temperature and pressure

* Corresponding author.
E-mail address: gerald.jomard@cea.fr (G. Jomard).

0022-3115/$ - see front matter © 2007 Elsevier B.V. All rights reserved.
doi:10.1016/j.jnucmat.2007.09.012

encountered along dynamics, each stable state experimentally observed in the conditions of the dynamics. In the case of plutonium, such a potential must be able to model six equilibrium solid phases as well as the liquid one as a function of temperature at zero pressure. The success in developing a reliable potential was first reached by Baskes within the modified embedded atom (MEAM) framework [14–16]. In the present work, we used this pure plutonium MEAM potential to predict the damage production induced by collision cascades in the face-centered-cubic δ-Pu for standard temperature and pressure conditions (SPT). We found that this very unusual element does not seem to behave like other fcc metals under irradiation. The origin of this discrepancy is not yet well understood, but as Valone et al., we argue that its origin could be linked to the coexistence of many structural phases (such as the monoclinic α-Pu and the δ-Pu ones) on the MEAM potential energy surface. As we will see in the following this seems to be confirmed by the simulations we performed with a simpler EAM interatomic potential which is only able to describe the δ and the liquid phases. With such an interatomic model, the damage production caused by self-irradiation in plutonium is similar to what is known for other fcc metals. This result emphasizes the fact that in MD simulations the formalism describing the interactions must be chosen with great care.

After a brief description of the potential, the conditions of our simulations are exposed. The displacement cascades results are then reported and discussed regarding modelling parameters, before to conclude.

2. Interatomic potential

The time evolution of a displacement cascade can be divided into two main stages. The first one is dominated by collision sequences. During this stage, the primary knock on atom (PKA) energy is distributed to other atoms. It stops when no atom can reach a sufficiently high energy to leave its lattice site. The result of this stage is the formation of a melted core. During the following stage, the cascade core relaxes to an equilibrium configuration with respect to temperature and pressure. Recently, Baskes and coworkers published a MEAM potential that is able to reproduce the (P,T) phase diagram of Pu [14,15]. It especially predicts the correct sequence of the six solid phases adopted from 0 K up to the melting. Moreover, mechanical constants, bulk modulus as well as negative Cauchy pressure ($P_c = 1/2(C_{12} - C_{44})$) of δ plutonium are correctly captured in this formalism whereas the simpler EAM potential was shown to be unsuitable to reproduce these properties [14]. This point could be the source of the poor description of the interactions obtained when the more attractive, less time-consuming analytical EAM formalism is used. That justifies the choice for the MEAM potential to describe self-irradiation damages creation in plutonium.

In both EAM and MEAM formalisms, the total energy of a set of particles is given by:

$$E = \sum_i \left(F(\bar{\rho}_i) + \frac{1}{2} \sum_{j \neq i} \Phi(r_{ij}) \right), \tag{1}$$

where $F(\bar{\rho}_i)$ is the attractive embedding function and $\Phi(r_{ij})$ the pair repulsive potential with r_{ij} the distance between atoms i and j [14].

In (1) $\bar{\rho}_i$ is the background electron density at position of atom i. The main difference between EAM and MEAM formalisms resides in the analytical expression of $\bar{\rho}_i$. Whereas the EAM background electronic density on the ith atom is formally spherical, within MEAM it results from a combination of angularly-dependent partial electronic densities:

$$\bar{\rho}_i = \rho_i^{(0)} \frac{2}{1 + \exp(-\Gamma_i)}, \tag{2}$$

where Γ_i contains the angular effects of the bonding:

$$\Gamma_i = \sum_{l=1}^{3} t_i^{(l)} \left[\frac{\rho_i^{(l)}}{\rho_i^{(0)}} \right]^2, \tag{3}$$

with $\rho_i^{(l)}$ being the partial electronic densities on atom i and $t_i^{(l)}$ their weights.

This formulation of $\bar{\rho}_i$ makes energy to depend not only on interatomic distances but also on atomic relative positions and spatial organization. This allows to capture the physical properties of a great number of structural phases even with a first nearest neighbors model. Let us mention here that, as in the formulation of Baskes [16], a radial cutoff function is applied to all radial functions. In addition an angular screening as defined in Ref. [17] has been used with the standard values given by Baskes for plutonium [16]. In agreement with Baskes, we found that the choice of radial cutoff does not significantly affect any of the results presented in this paper. However we must mention that we did not test another angular screening formulation as the one proposed by Baskes, Angelo and Bisson [17]. We are thus unable to discuss of the incidence of this choice to our predictions. If the angular screening parameters published in Ref. [16] seem to be well defined for the crystalline phases of plutonium, Cherne et al. found that it is less clear for the liquid state as the melting points are affected by the choice of the $C_{\min}$ parameter [18,19]. We may thus expect that varying this parameter in our simulations would have certainly slightly modify our results. But such a modification would also have modified the melting temperature which is correctly predicted with $C_{\min} = 2.0$, it is why we have preferred to leave it unchanged.

One may note that high energy cascades involve, in the above-mentioned collision stage, close distance interactions that are not correctly taken into account by the original potential of Baskes [16]. We have thus adopted the usual solution consisting in adding a short range ionic repulsive core to the potential. For that purpose we developed a special adaptation of this method to the N-body MEAM formalism. The repulsive part of the potential has been modified to provide a better treatment of atomic interactions

below the smallest equilibrium neighbor distance which is 2.5 Å in the α-Pu monoclinic crystallograhic phase. An ionic repulsive core was smoothly joined to the repulsive potential, Φ, with an exponential of a polynomial of the third order between 1 and 2 Å:

$$\begin{aligned} &r \leqslant r_{\text{inf}} \Phi(r) = \Phi_{\text{KrC}}(r) \\ &r_{\text{inf}} < r \leqslant r_{\text{sup}} \Phi(r) = \exp\left(a_0 + a_1 r + a_2 r^2 + a_3 r^3\right), \\ &r > r_{\text{sup}} \Phi(r) = \Phi_{\text{MEAM}}(r) \end{aligned} \tag{4}$$

where $r_{\text{inf}} = 1$ Å, $r_{\text{sup}} = 2$ Å, $\Phi_{\text{MEAM}}(r)$ is the repulsive part of MEAM potential in (1), $\Phi_{\text{KrC}}(r)$ is the universal Kr-C potential of Wilson et al. [20] and a_i with $i = 0,\ldots 3$ are chosen to ensure the continuity of Φ and its derivatives. The Kr-C potential of Wilson et al. is expressed as a Coulombic $(1/r)$ term multiplied by a "screening" function; interatomic distances are expressed in units of a screening length. In this way, the interaction can be universaly applied if the screening function is known. The screening function is parametrized by a sum of exponentials, the corresponding parameters are determined from least-squares fit to ab initio calculated free-electron potentials for various systems. More details about this universal potential can be found in the original paper of Wilson et al. [20]. Since the Kr-C potential only applies for small interatomic distances we have not considered any radial cut-off or angular screening like the ones discussed in the following for the MEAM part of the interaction. Dremov and coworkers studied the effect of the form of the strengthening potential at small interatomic distances [21,22] on the average displacement energy. They found that the result is not sensitive to the potential used, we are thus quite confident in our choice.

In the case of the background electronic density, $\bar{\rho}$ is progressively turned into its spherical contribution $\rho^{(0)}$ as interatomic distance decreases. The following expressions are obtained for the partial electronic densities:

$$\begin{aligned} &r \leqslant r^{\rho}_{\text{inf}} \quad \begin{cases} \rho^{(0)} = \frac{Z}{4\pi r} \frac{\mathrm{d}^2 \Phi}{\mathrm{d}r^2} \\ \rho^{(l)} = 0 \qquad \text{for} \quad l = 1,\ldots 3 \end{cases} \\ &r^{\rho}_{\text{inf}} < r \leqslant r^{\rho}_{\text{sup}} \begin{cases} \rho^{(0)} = \exp\left(a_0 + a_1 r + a_2 r^2 + a_3 r^3\right) \\ \rho^{(l)} = \rho^{(l)}_{\text{MEAM}} \times f_c(r) \\ \text{for} \quad l = 1,\ldots 3 \end{cases} \\ &r > r^{\rho}_{\text{sup}} \quad \rho^{(l)} = \rho^{(l)}_{\text{MEAM}} \quad \text{for} \quad l = 0,\ldots 3 \end{aligned} \tag{5}$$

where $r^{\rho}_{\text{inf}} = 1$ Å, $r^{\rho}_{\text{sup}} = 2.5$Å,

$$f_c(r) = \left(1 - \left(1 - \frac{r - r^{\rho}_{\text{inf}}}{r^{\rho}_{\text{sup}} - r^{\rho}_{\text{inf}}}\right)^2\right)^4 \tag{6}$$

is a cutoff function smoothly going from 0 to 1 when r goes from r^{ρ}_{inf} to r^{ρ}_{sup}.

The approach exposed in (5) is based on the fact that at small distances atomic electronic density distribution is close to the sphere, and angular contributions, $\rho^{(l)}(r)$ for $l = 1,\ldots 3$, tend to zero when $r \to 0$. The resulting hardening allows collision cascade simulations with energy up to 80 keV. This hardening is taken into account for very close interatomic distances and does not affect equilibrium properties.

3. Computational method

To model the defects production by MD, a fcc crystal of plutonium is first built and equilibrated for 10 ps in the statistical microcanonic ensemble (NVE) in order to reach a final mean temperature value of 300 K. The δ phase of plutonium is not stable at room temperature (RT) with the MEAM potential. However, as explained by Valone and Baskes, the constant volume simulation box, retaining its shape, allows one to stabilize the fcc lattice configuration down to 300 K [23]. Valone and co-workers, found that volume stabilization is not maintained for large cells [24]. In our simulations we never encountered such a situation. The only difference between our approach and the one of Valone et al. is the use of the function $G(\Gamma) = 2/(1 + \exp(-\Gamma))$ instead of $G(\Gamma) = \sqrt{(1 + \Gamma)}$ in the construction of the background electron density $\bar{\rho}_i$. We have checked that with this later function our results were unchanged so we have currently no explanation for this discrepancy.

During the plutonium α-decay process both uranium and helium nuclei are emitted in the metal. These particles transfer their kinetic energy to the material through collision sequences creating structural defects. Most of these defects are produced by the uranium nucleus carrying about 64 keV available for cascades [2]. The α particle yielding more than 99% of its energy to electrons is not considered in the calculations. An atom near the center of the simulation cell is then selected to simulate the uranium which is the PKA in our calculations. A kinetic energy, in an arbitrary crystallographic direction, is given to this atom to model the displacement cascade of interest.

The size of the simulation cell has been adjusted in such a way that the equipartition of the PKA energy in kinetic and potential modes corresponds to 10 K/atom:

$$E_{\text{PKA}} = 3Nk\Delta T, \tag{7}$$

with E_{PKA} the displacement cascade energy, k the Boltzmann constant, $\Delta T = 10$ K the mean temperature increase and N the number of atoms. Applying (7) one gets the size of the simulation cell versus cascade energy as given in Table 1.

Displacement cascades simulations were performed with periodic boundary conditions. The equations of motion are solved with an adaptative method in which the time step is adjusted to the fastest atom:

Table 1
Size of simulation cell size versus PKA energy

E_{PKA} (keV)	1	2	5	10	60
N	386 473	772 946	1 932 367	3 864 734	23 188 406

$$\delta t = \frac{a_0}{3000 v_{\max}}, \quad (8)$$

with a_0 the lattice parameter of the δ-Pu phase and $v_{\max}$ the fastest atom velocity. This approach, limiting long distance displacement between two steps and reducing number of integration steps as the dynamics slows down, ensures a perfect energy conservation and contributes to minimize the computational effort.

Point defects were defined thanks to Voronoi cells method on fcc lattice sites.

The calculations have been performed on 64 processors of the TERA supercomputer of the CEA/DAM using the MD code STAMP developed at CEA/DPTA/SPMC [25].

4. Results

In a previous work, an EAM potential has been used to study self-irradiation effects in plutonium [26]. As explained before the EAM formalism is not able to reproduce plutonium elastic constants and MEAM potential was preferred as a more confident approach. However it is interesting to compare collision cascades evolution given by these two models. In this way, we have started this work by performing 2 keV displacement cascades simulations, with both potentials, in the same conditions as those used by Pochet [26]. Next, having a larger knowledge of the dynamics in MEAM, 10 keV collision sequences have been initiated with different conditions to determine their consequences on the dynamic. In this section, we present results on threshold displacement energies calculations together with 2 keV and 10 keV collision cascades simulations.

4.1. Threshold displacement energy

Threshold displacement energy, E_d, has been first computed to measure the effect of the potential hardening on this property. The procedure for the calculation was the same as for collision cascades. In a simulation cell of 32000 atoms a small energy displacement cascade was initiated for 15 ps in the direction of interest. The number of vacancy created during the process was checked. If no stable defect remained at the end of the simulation, the PKA energy was increased by 1 eV for a new calculation. The procedure was iterated until at least one stable Frenkel pair was obtained. Displacement threshold energies computed by this method are reported in Table 2.

Except for directions of high density ($\langle 100\rangle$, $\langle 110\rangle$, $\langle 111\rangle$), the threshold displacement energy is about 5–6 eV. High density direction leading to replacement collision sequences are not representative of displacement cascade process. This is why an average value of 6 eV for E_d is retained. This value is in perfect agreement with linear interpolation of E_d from low energy cascades displacement calculations reported by Valone et al. [23]. One should note that despite the hardening of the potential, the threshold energy for plutonium in the MEAM formalism is obviously small. For comparison, estimations from sublimation enthalpy or melting temperature gives 33 and 14 eV [23] respectively. Our prediction is well below these two estimations. This may be a consequence of local minima surrounding fcc positions within the MEAM model. These minima would be a manifestation of the multi-phase property of the potential. The minima stabilizing Frenkel pair could lead to an underestimated threshold energy. Thus, Valone claimed that this low value for E_d is due to the metastability of the delta phase and argued that a 10 eV value would be preferable [23]. Experimental plutonium resistivity measurements under irradiation are currently performed to settle the question on the amplitude of E_d. These measurements will then be used to fit new potentials.

4.2. Displacement cascades

4.2.1. 2 keV cascades simulations

To compare EAM and MEAM formalisms, 2 keV displacement cascades were simulated in a cubic $60a_0 \times 60a_0 \times 60a_0$ box of 864000 atoms. The size of the simulation cell, defined by Pochet [26], limits ΔT to 9 K with respect to the criterion given in (7). The PKA directions were set to $\langle 421\rangle$ and $\langle 513\rangle$. No control of the temperature was applied during the first 200 ps. After 200 ps, the collision stage was finished and the PKA energy was completely distributed over degrees of freedom of the system. A Nosé-Hoover thermostat was then applied to reach complete equilibration of the damaged structure at the chosen temperature. The thermostat has been set to 300 K to mimic the dispersion of excess temperature due to the PKA in a real macroscopic system and to 600 K to accelerate the damage relaxation kinetics. The temperature increase was then explored as a method to speed up the defect recombination rate during the relaxation stage. The evolution of the number of vacancies during the first 200 ps is reported on Figs. 1 and 2. Both cascades have similar behavior with an increase in the number of vacancies during the ballistic phase, followed by a decrease during the cooling stage and stabilisation in a further relaxation stage. However dynamics are quite different from previous results from Pochet [26] or usual fcc metals [7,9]. The number of vacancies is maximum after 1.8 ps for the two directions when Pochet reported 3–4 ps. The cooling stage lasts about 10 ps which is not that different from

Table 2
Displacement threshold energy versus crystallographic direction evaluated using hardened MEAM potential

Direction	$\langle 100\rangle$	$\langle 110\rangle$	$\langle 111\rangle$	$\langle 120\rangle$	$\langle 320\rangle$	$\langle 321\rangle$	$\langle 421\rangle$	$\langle 513\rangle$	$\langle 1025\rangle$
E_d	13	9	11	5	6	6	5	6	5

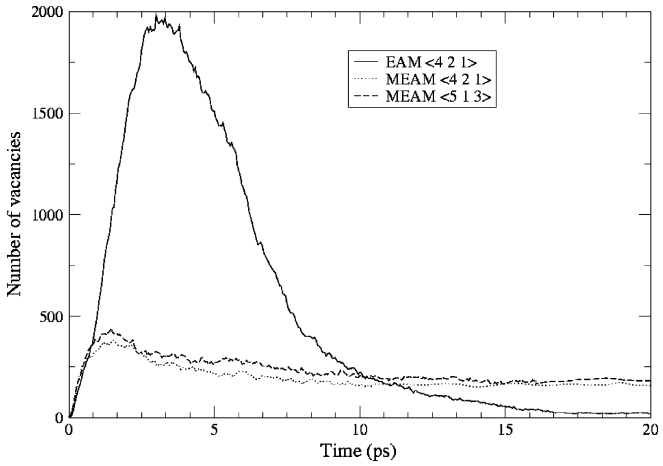

Fig. 1. Number of vacancies as a function of time during the first 20 ps of 2 keV displacement cascade simulations in EAM and MEAM potentials.

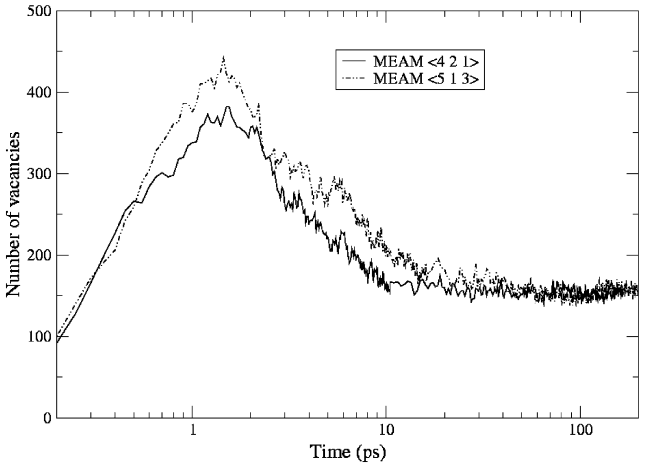

Fig. 2. Number of vacancies as a function of time during 2 keV displacement cascade simulations in MEAM potential: calculation to 200 ps.

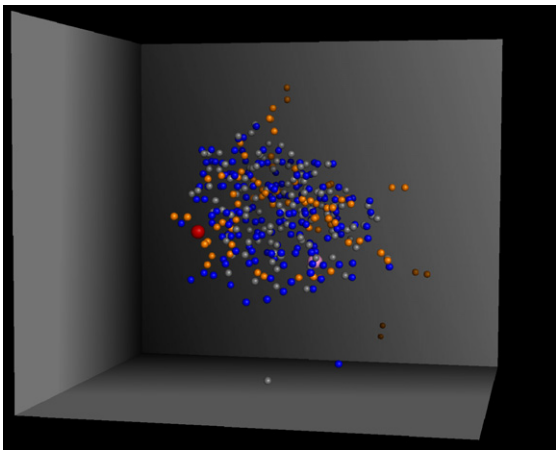

Fig. 3. Defects microstructure representation for ⟨513⟩ MEAM simulation at 200 ps: Vacancies (blue), self-interstitials (grey) and dumbbells (orange). The initial position of the PKA is shown in red and its final position in purple. (For interpretation of the references to colour in this figure legend, the reader is referred to the web version of this article.)

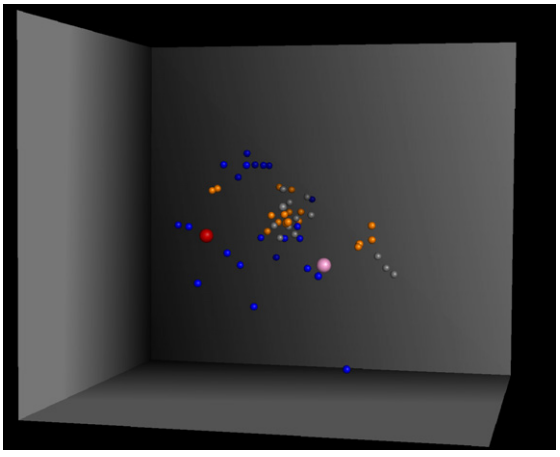

Fig. 4. Defects microstructure representation for ⟨513⟩ MEAM simulation at 15 ns: Vacancies (blue), self-interstitials (grey) and dumbbells (orange). The initial position of the PKA is shown in red and its final position in purple. (For interpretation of the references to colour in this figure legend, the reader is referred to the web version of this article.)

EAM or fcc metals, but the relaxation stage takes place over nanoseconds. Almost 15 ns are required to reach complete annealing of the cascade core which is far more than for usual materials or plutonium described by an EAM model.

About 400 vacancies were created at the ballistic peak which is ten times lower than for the EAM potential. The number of vacancies remained stable to 160 for the two directions, decreasing slowly to reach 20 in the final structure after 15 ns. Point defects microstructures for 200 ps and 15 ns are shown on Figs. 3 and 4.

Cascades cores which radius is around 10–18 Å, reveal the formation of an amorphous region with isolated surrounding interstitials produced by replacement collision sequences. At the end of the relaxation stage, no vacancy cluster is observed and only small interstitials clusters of two to six atoms are formed.

The orientation of dumbbells has been studied in details. On Figs. 5 and 6 the coordinates of the unitary vector along dumbbell axis have been reported. The resulting points lie at the surface of a spherical sector located between (xOy), (yOz) and (zOx) planes. The corners of the figure correspond to ⟨100⟩ orientation of the clusters, the middle of the edges to ⟨110⟩ and the center to ⟨111⟩. A high density of points in one of these sectors would mean that clusters adopt a specific orientation. Fig. 5 shows that after 200 ps of simulation, dumbbells do not exhibit any specific orientation. On contrary, Fig. 6 shows that at the end of the relaxation stage, di-interstitials are ⟨100⟩ dumbbells with interatomic distance of 2.5 ± 0.1 Å, some being ⟨111⟩. This result is in agreement with what has been reported by Valone and coworkers and with our calculated formation energies which indicate that the ⟨100⟩ split interstitials are the most favored ones [23,27]. Indeed, according to our simulations, the formation energy of the ⟨100⟩ split

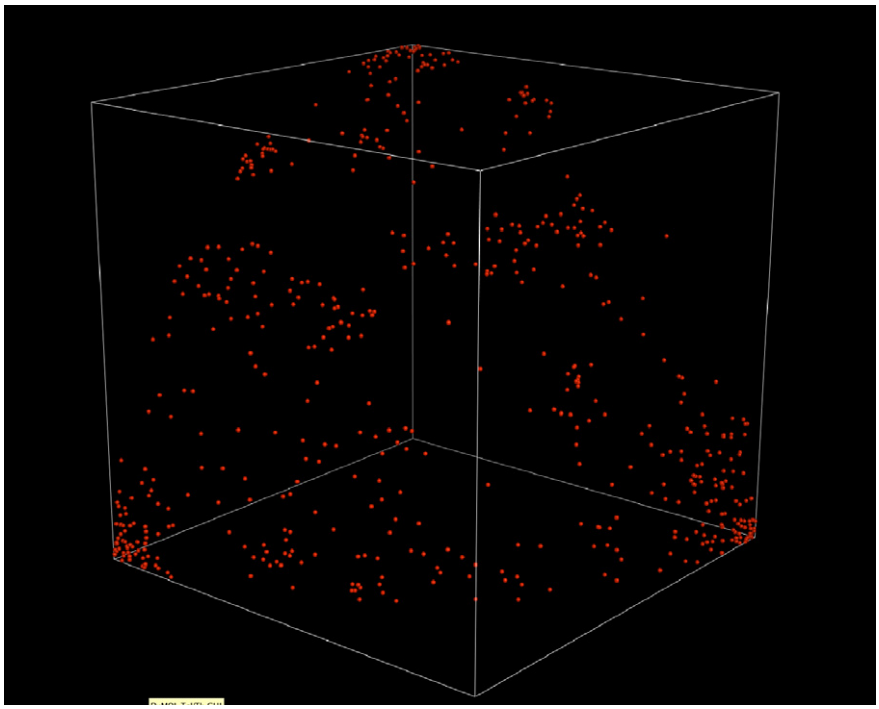

Fig. 5. Two bodies interstitials clusters orientation at 200 ps.

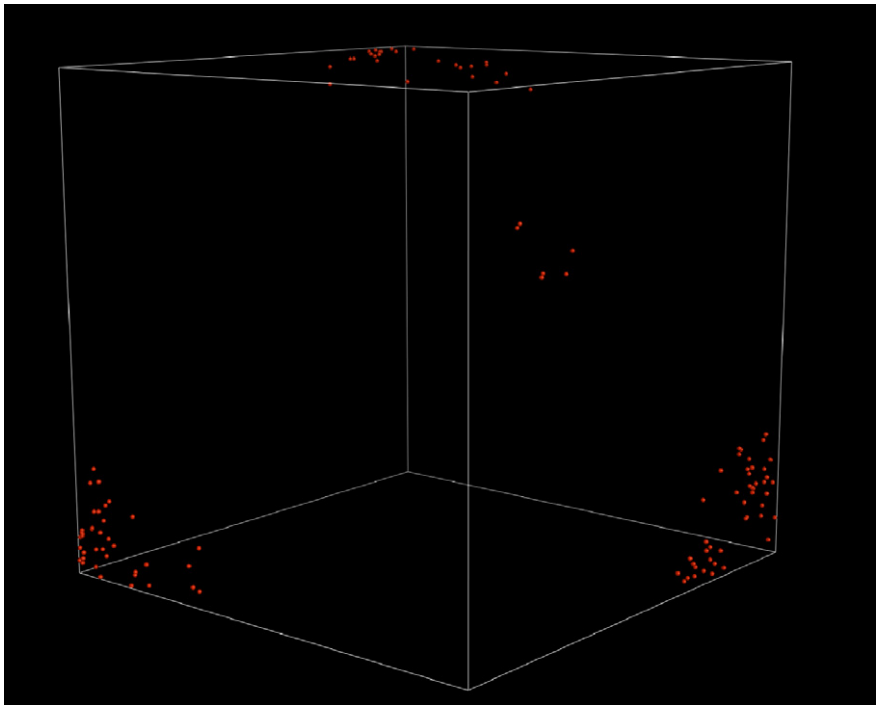

Fig. 6. Two bodies interstitials clusters orientation at 15 ns.

interstitials is around 0.5 eV, that is much lower than for the other orientations for which the formation energy ranges from 1.2 to 1.4 eV.

Doing similar calculations with an EAM potential, Pochet observed the formation of a 50-vacancy microvoid near the center of the cascade and two principal interstitials clusters of 20 elements which remain stable after only 50 ps. The point defects calculated formation energies with this EAM potential also indicate that the $\langle 1\,0\,0 \rangle$ are the most energetically favored but the energy differences between each type of interstitials are not so high as with the MEAM potential [28]. The results exposed in this paper point out

the fact that EAM and MEAM methods lead to significantly different results due to the description of atomic interactions. We performed displacement cascades simulation in Cu with MEAM formalism that have proven that the dynamic behavior is not simply a consequence of the potential but rather due to the coexisting plutonium α and δ phases on potential surface energy. These observations show that irradiation effects in plutonium are quite different than in other metals and that quality of interatomic potential can significantly modify MD simulation results.

4.2.2. 10 keV cascades simulations

To investigate the effect of displacement cascade energy on dynamic behavior and point defect production, 10 keV collision sequences have been performed in plutonium in directions $\langle 4\,2\,1\rangle$, $\langle 5\,1\,3\rangle$ and $\langle 1\,0\,2\,5\rangle$. Except for the simulation cell size, calculations have been dimensioned as described previously. The simulation cell had to be large enough to contain the entire cascade region and to avoid self-interaction because of periodic boundary conditions. The strict respect of the criterion given in (7) leads to a simulation box of $100\times100\times100$ unit cells. The resulting crystal of four million atoms looks perfectly adapted to capture most 10 keV displacement cascades. But considering Eq. (8) with $E_{PKA}=10$ keV, it appears that the simulation of such a cascade requires $\delta t\sim2\times10^{-6}$ ps and then involves millions of time steps to reach the ballistic peak. Then to save CPU time, smaller simulation cells were used. In [26], Pochet mentioned that a pressure wave due to the cascade travels in the system through periodic conditions. He argued that this pressure wave would perturbed the cascade relaxation if the simulation cell is too small. Thus to measure the effect of the simulation cell size, 10 keV displacement cascades were initiated in 2048000 and 864000 atoms cells.

Evolutions of the number of vacancies produced during simulation of 10 keV displacement cascades with the two box sizes are reported on Figs. 7 and 8. These figures show that the number of vacancies was qualitatively the same whatever the PKA direction and the simulation cell size. The ballistic peak occured between 2.4 and 2.9 ps. The vacancies number ranging from 3500 to 4800 was ten times larger than for 2 keV simulations. At the end of the cooling stage which lasted about 10 ps, 2000 vacancies remained in the crystal. This number decreases slowly to reach 1600 vacancies at 200 ps and 1 500 at 2 ns. It continues to decrease by 40 vacancies per nanosecond during the following 3 ns. The cascade core evolves slowly and adopts a glassy-like structure with a radius of 28 Å.

Crystallization of the perturbed region in a more stable solid phase than the fcc plutonium δ phase could be cited to explain the long lifetime of cascades core observed within the MEAM potential. The calculation of pair distribution functions (PDF) shows that interstitials are strongly relaxed in the direction of vacancies with an interstitial-vacancy separation distance of about 1.8 Å when the radius

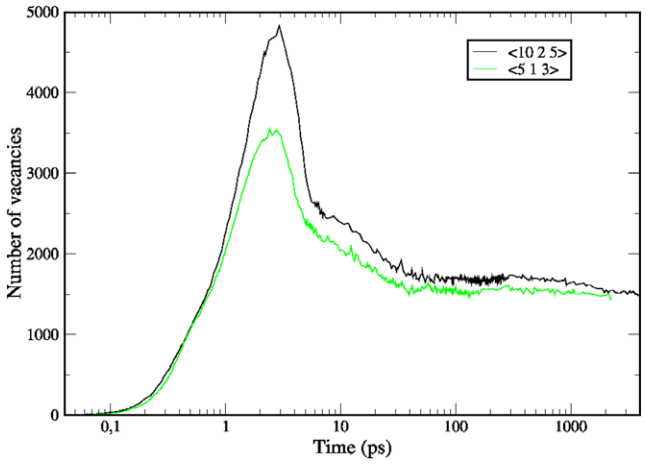

Fig. 7. Number of vacancies versus time during 10 keV displacement cascade simulations with MEAM potentials in 864000 atoms.

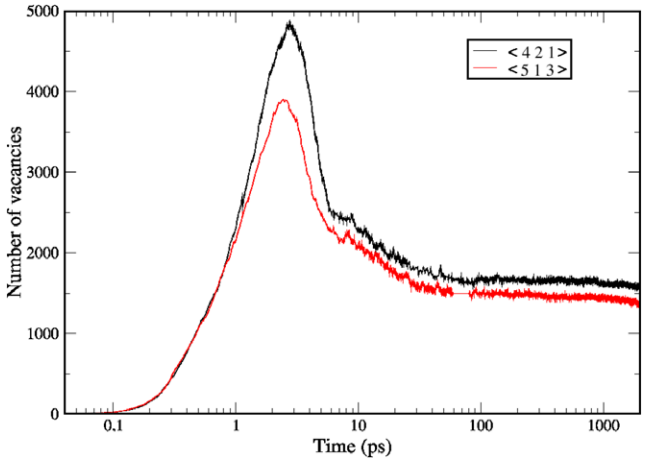

Fig. 8. Number of vacancies versus time during 10 keV displacement cascade simulations with MEAM potentials in 2048000 atoms.

of octahedral and tetrahedral fcc sites are 2.3 and 2.0 Å. Dumbbells are in the vicinity of the vacancies (at more or less 2 Å), their interatomic distances are distributed between 2.4 and 3.2 Å. Dumbbells are randomly orientated with no specific direction for simulation times as long as 2 ns. Interstitial and dumbbell PDFs are liquid-like. No global order appears for interstitials and dumbbells populations. We performed a local structure search through PDF calculations including all the atoms located in and near the cascade cores. We analysed all clusters formed by such atoms, with the following definition: an atom is part of a cluster if its distance from an existing cluster is in between 2.5 and 2.9 Å. No order was found on these clusters. PDF evaluation proved that microstructure defect stability can not be attributed either to the occurence of any plutonium solid phase in the cascade core or to the presence of some microcrystal of another solid phase than fcc in clusters.

To summarize, our cascade simulation results and PDF calculations show that cascade core region exhibits a

liquid-like structure of high metastability. If one wants to explain this stability by the nature of the potential possessing numerous minima around fcc positions, he has to admit that these minima stabilize not only plutonium solid phases but also a disordered liquid phase in SPT. Another explanation could lie in the short range of the MEAM potential in which interactions are cut after 4.5 Å. As mentioned by Baskes [16], in MEAM, the phase stability is determined by nearest-neighbor interactions. One way to ensure that our observations are linked to the uncommon physics of plutonium rather than to the use of an artificially metastablized delta phase, would be to perform simulations with a thermodynamically stabilized FCC phase by using the PuGa MEAM potential of Baskes et al. [24]. Indeed, this potential is able to reproduce the delta-phase stabilization by addition of small amounts of Ga in the Pu metal in agreement with experimental observations. Then one can perfomed simulations in SPT conditions on a phase stabilized by alloying effects rather than by a volume constraint. Recently, Dremov and co-workers had used the above-mentioned PuGa potential parametrized by Baskes et al. [24] in a mixed Monte-Carlo and molecular dynamics simulation study of radiation damage evolution in Pu [22]. Their simulations showed that the formation of amorphous (melted) region is proper to the cascade evolution in pure and alloyed Pu. Their conclusion suggests that our observations are not linked to the volume constraint used in our simulations but rather to the physics of plutonium. In cascade, the bulk fcc structure drives the relaxation of the crystal to the plutonium δ phase. Atoms near the center of the cascade are beyond the force field of the bulk and are subject to disorder interactions. Thus the cascade relaxation would progress step by step from the edge to the center of the amorphous region, the presence of local minima slowing down the kinetics. Such a recombination of defects would take place over long time scale at the limits of MD possibilities (i.e. dozens of ns). A consequence of this hypothesis would be a complete amorphization in case of a simulation cell that is too small in comparison to the perturbation introduced by the cascade, or in case of a lack of stability of the initial configuration due to temperature or pressure conditions. In both cases the crystal would not be able to drive the relaxation and the perturbation would spread over the simulation cell. The apparent stability of defects population probably has several origins which come from the exotic properties of plutonium, the analytical form of the MEAM potential as well as its short range interactions cutoff and angular screening.

A linear interpolation of the number of vacancies based on 20 Frenkel pairs produced by 2 keV cascades leads to 100 remaining vacancies at the end of the relaxation stage of 10 keV cascades. Taking a constant recombination rate of 40 vacancies per nanoseconds one estimates to 40 ns the MD time to reach the complete relaxation of the cascade. This is far from what we are able to do in a decent human time.

4.2.3. Kinetic rate improvement

In our plutonium aging simulation program, the goal of the MD cascades simulations is to provide defect poulations statistically representative of damage produced by self-irradiation in plutonium to mesoscopic scale codes.

Simulation of displacement cascades in plutonium with MEAM potential are very time-consuming as shown previously. That prevents from the accumulation of such calculations which are required to understand intrinsic properties defining plutonium α-decay defects microstructures. This is why the rise up of temperature was explored as a technique to accelerate the kinetic rate during the relaxation stage of cascades. Fig. 9 shows the evolution of the number of vacancies when setting the thermostat temperature to 600 K after 200 ps. It depicts that rising the temperature from 300 K to 600 K can increase the relaxation kinetic rate by a factor of about 50 for 2 keV cascades. This is justified both by the fact that δ-Pu is stable at 600 K (consequently the recrystallisation of the disordered core of the cascades is favored) and by the fact that at this higher temperature, the migration of the point defects is favored, the probability of recombination is then increased.

The remaining number of vacancies is about 16, that is in agreement with what is found at $T = 300$ K. Moreover, vacancies spatial repartition is similar for both temperature (see Figs. 10 and 11).

We also checked that the dumbbells orientation is independent of the temperature (i.e. $\langle 1\,0\,0 \rangle$). However the spatial repartition of this kind of defects obtained after an increase of the temperature is very different from what is observed in SPT. When at 300 K small interstitials clusters remained, only self-interstitials or dumbbells subsist at the end of the simulation at 600 K. In addition, interstitials have migrated far from the cascade core. This last result is not surprising considering the very small migration energy of such species [23,27]. As mentioned earlier, displacement cascade simulations results: defects number,

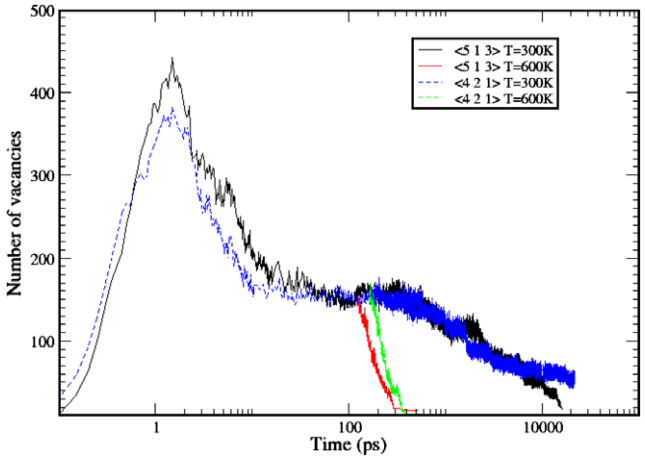

Fig. 9. Comparison of vacancies number evolution during 300 K and 600 K relaxation stage.

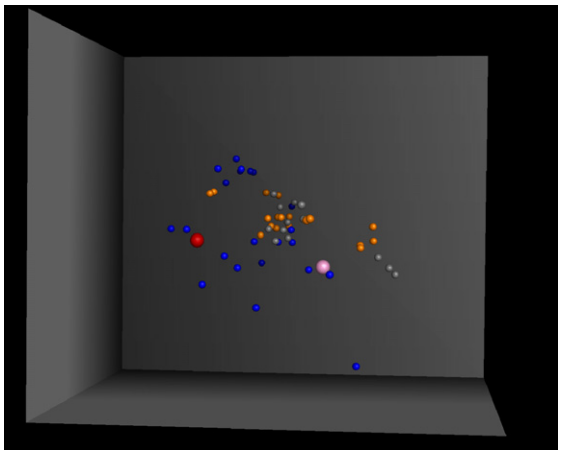

Fig. 10. Final defects microstructure for ⟨513⟩ MEAM simulation at 300 K. Vacancies are represented in blue, self-interstitials in grey and dumbbells in orange(*). (For interpretation of the references to colour in this figure legend, the reader is referred to the web version of this article.)

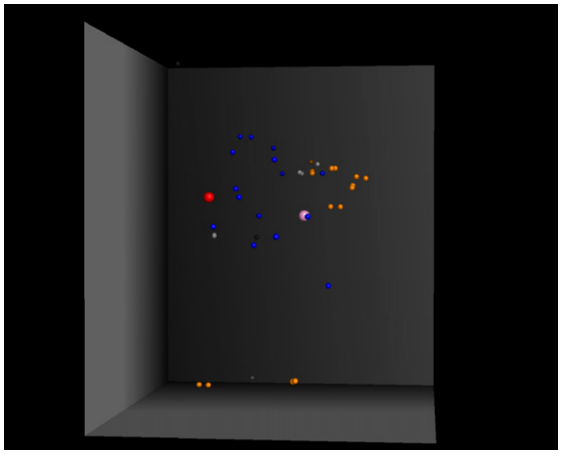

Fig. 11. Final defects microstructure for ⟨513⟩ MEAM simulation at 600 K. Vacancies are represented in blue, self-interstitials in grey and dumbbells in orange(*). The initial position of the PKA is shown in red and its final position in purple. (*) Colors should be adapted to journal requirements). (For interpretation of the references to colour in this figure legend, the reader is referred to the web version of this article.)

spatial repartition, cluster size and formation energies are used as input data for our Monte-Carlo mesoscopic scale simulations. Recent calculations show that MC simulations are sensitive to spatial correlation of defects [29]. Consequently, the rise up of temperature, modifying spatial distribution of defects, does not constitute a confident method to accelerate defects microstructure relaxation and save CPU time.

5. Discussions

The study of 2 keV and 10 keV displacement cascades in fcc plutonium has been performed using a MEAM potential for pure plutonium metal. This potential has first been hardened to reach physical modelling of short range interactions involved in collision sequences. It was shown that this hardening did not significantly modify equilibrium properties as well as threshold displacement energy which was found to be about 6 eV. It was mentioned that such a value for E_d seems very small for plutonium and is probably a consequence of local minima surrounding fcc positions due to the multi-phase behavior of the Pu MEAM potential. Setting $t^{(3)}$ to zero in the combination of electronic densities $\Gamma = \sum_{i=1,3} t^{(i)}(\rho^{(i)}/\rho^{(0)})^2$, Valone has obtained the so-called MEAM* potential which artificially imposes the fcc phase as the ground state for plutonium. In these conditions, he reports a value of 16 eV for the threshold displacement energy. This value looks more acceptable, but the behavior of this modified potential in self-irradiation process is still not clear. Kubota has performed displacement cascades simulations with this model and shows that it strongly changes the results. The consequence is that plutonium behaves more like usual fcc metals under irradiation [30]. The evolution of the number of vacancies is then similar to the EAM results [26] but a detail comparison between her simulations in MEAM* and EAM ones has not been done yet. In usual fcc metals, vacancies tend to diffuse and form clusters. With an EAM potential for plutonium, Pochet observed this tendency [26] but this is not the case with MEAM potential. In the last case most of the vacancies were isolated and only small vacancy clusters of 2 or 3 bodies were obtained.

It is currently clear that interatomic potential formalism can affect considerably displacement cascades results. The present-day tendency is to improve the potential to reach an efficient representation of plutonium alloys properties. First principal calculations and experimental measurements are currently used to determined mechanical properties and relative phase stability which are essential input data for classical interatomic potential development. Potentials allowing one to capture cohesive and structural properties of Pu-Ga systems already exist but they have not yet been used to study high energy cascades in such alloys [31,24]. These potentials are able to reproduce the δ-phase stabilization by addition of small amounts of gallium in plutonium at room temperature. Thus, it is now possible to simulate collision cascades in SPT in a thermodynamically stable δ-PuGa alloy. Such study would be of great interest in order to check if the remarkable results obtained in this work with a pure plutonium MEAM potential are only due to the use of the model away form its range of validity.

References

[1] O. Chebotarev, O. Utkina, Plutonium and other actinides, vol. 599, North-Holland Publishing Company, 1976.
[2] W.G. Wolfer, Los Alamos Sci. 26 (2000) 275.
[3] B. Oudot, PhD thesis, Université de Franche Comté, 2005.
[4] N. Baclet, P. Faure, G. Rosa, B. Ravat, L. Jolly, B. Oudot, L. Berlu, V. Klosek, J.L. Flament, and G. Jomard, Understanding and predicting self-irradiation effects in plutonium alloys: A coupled experimental and theoretical approach, In Actinides 2005, 2005.

[5] L. Berlu, P. Faure, G. Rosa, and G. Jomard, in: J. Sarrao, A. Schwartz, M. Antonio, P. Burns, R. Haire, and H. Nische (Eds.), Basis Science, Application and Technology, vol. 893, Warrendale, 2005. Mater. Res. Symp. Proc, PA.
[6] W.J. Phythian, R.E. Stoller, A.J.E. Foreman, A.F. Calder, D.J. Bacon, J. Nucl. Mater. 223 (1995) 245.
[7] D.J. Bacon, A.F. Calder, F. Gao, J. Nucl. Mater. 251 (1997) 1.
[8] L. Malerba, J. Nucl. Mater. 351 (2006) 1.
[9] D.J. Bacon, F. Gao, Yu N. Osetsky, J. Nucl. Mater. 276 (2000) 1.
[10] Yu N. Osetsky, D.J. Bacon, Nucl. Instr. Meth. Phys. Res. B 180 (2001) 85.
[11] M. Hou, D. Kulikov, J. Nucl. Mater. 336 (2005) 25.
[12] H.L. Heinisch, W.J. Weber, Nucl. Instr. Meth. Phys. Res. B 228 (2005) 293.
[13] R.E. Voskoboinikov, Yu N. Osetsky, D.J. Bacon, Nucl. Instr. Meth. Phys. Res. B 242 (2006) 68.
[14] M.S. Daw, M.I. Baskes, Phys. Rev. B 29 (1984) 6643.
[15] M.I. Baskes, Phys. Rev. B 46 (1992) 2727.
[16] M.I. Baskes, Phys. Rev. B 62 (2000) 15532.
[17] M.I. Baskes, J.E. Angelo, C.L. Bisson, Modell. Simul. Mater. Sci. Eng. 2 (1994) 505.
[18] F.J. Cherne, M.I. Baskes, P.A. Deymier, Phys. Rev. B 65 (2001) 024209.
[19] F.J. Cherne, M.I. Baskes, B.L. Holian, Phys. Rev. B 67 (2003) 092104.
[20] W.D. Wilson, L.G. Haggmark, J.P. Biersack, Phys. Rev. B 15 (1977) 2458.
[21] V.V. Dremov, Private Communication.
[22] V.V. Dremov, F.A. Sapozhnikov, S.I. Samarin, D.G. Modestov, N.E. Chizhkova, J. Alloys Compd. 444 (2007) 197.
[23] S.M. Valone, M.I. Baskes, M. Stam, T.E. Mitchell, A.C. Lawson, K.E. Sickafus, J. Nucl. Mater. 324 (2004) 41.
[24] S.M. Valone, M.I. Baskes, R.L. Martin, Phys. Rev. B 73 (2006) 214209.
[25] J.P. Ansart, G. Jomard, B. Magne, J.B. Maillet, L. Soulard, G. Zérah, User's manual for the code STAMP. Technical report, CEA/DIF/DPTA/SMPC, 2001.
[26] P. Pochet, Nucl. Instrum. and Meth. Phys. Res. B 202 (2003) 82.
[27] L. Berlu, G. Jomard, G. Rosa, P. Faure, J. Nucl. Mater. (2006), doi:10.1016/j.jnucmat.2006.11.016.
[28] P. Pochet, Evaluation of the formation energy of point defects in δ-Pu with an eam potential. Private Communication.
[29] G. Jomard, L. Berlu, G. Rosa, P. Faure, J. Nadal, N. Baclet, Computer simulation study of self-irradiation in plutonium, J. Alloys Compd. 444–445 (2007) 310.
[30] A. Kubota, W.G. Wolfer, M.J. Caturla, Static and dynamic aspects of radiation damage in fcc plutonium from molecular dynamics simulation. 35ième journée des actinides, Vienna, Austria, unpublished results, 2005.
[31] M.I. Baskes, K. Muralidharan, M. Stan, S.M. Valone, F.J. Cherne, J.O.M. (September) (2003) 41.